Volume expansion of amorphous silicon electrodes during potentiostatic lithiation of Li-ion batteries

Harald Schmidt[a,b,*], Bujar Jerliu[a], Erwin Hüger[a], Jochen Stahn[c]

[a] *Technische Universität Clausthal, Institut für Metallurgie, AG Mikrokinetik, Clausthal-Zellerfeld, Germany*
[b] *Clausthaler Zentrum für Materialtechnik (CZM), Clausthal-Zellerfeld, Germany*
[c] *Laboratory for Neutron Scattering and Imaging, Paul Scherrer Institut, Villigen PSI, Switzerland*

ARTICLE INFO

ABSTRACT

Large volume modifications during electrochemical cycling of electrodes in Li-ion batteries often limit successful applications due to stress formation, electrode fracture and delamination from the current collector. In this study, we carried out investigations on the volume changes taking place during potentiostatic lithiation of the high capacity electrode material amorphous silicon. Thin film electrodes were investigated at potentials of 0.45, 0.28, 0.19 und 0.06 V vs Li/Li$^+$ during lithiation using in-operando neutron reflectometry. We found a strongly non-linear correlation between volume and state-of-charge for each potential applied in strong contrast to the results of galvanostatic lithiation. A possible explanation might be that for high current densities occurring at the beginning of each potentiostatic lithiation step free volumes are created in the electrode material leading to disproportionate volume expansion.

1. Introduction

A promising high capacity negative electrode material for Li-ion batteries is amorphous silicon with its high theoretical specific capacity of about 4000 mAh/g [1–4]. However, a stable long term performance is limited due to the enormous volume expansion up to about 400% where a high number of Li atoms are incorporated into the silicon electrode during lithiation [5]. This often has the consequence of a decay of specific capacity during cycling that is attributed to stress formation [6], mechanical fracture and irreversible side reactions that are invoked by the volume changes [2]. Consequently, the development of Si-based Li-ion batteries faces great challenges due to the volume changes induced by cycling and the correlated capacity fading. Some comprehensive reviews are given in [7,8]. In order to improve battery device operation, a precise measurement and improved fundamental understanding of volume changes taking place during lithiation is required, best by in-operando studies. In our previous work, an monotonic increase in volume during lithiation of amorphous silicon was measured by neutron reflectometry (NR) in-operando during galvanostatic cycling [5,9]. This increase is approximately linear for x > 0.5 assuming a Li$_x$Si layer formed during lithiation [5,9]. An increase in volume during lithiation was also observed by Atomic Force Microscopy [10–12], Synchrotron X-ray Imaging [13], Optical Diffraction Microscopy [14], X-ray Reflectivity [15] and by electron microscopy

during long term cycling [16]. A maximum expansion up to about 400% was found in agreement to our results and a linear change in volume after initial effects [5,9–11,14,15].

In the present study, we discuss in-operando neutron reflectometry experiments for the detection of volume changes occurring during potentiostatic lithiation not done before. In contrast to galvanostatic experiments, our results show a strongly non-linear correlation between volume and state-of-charge for each potential applied.

Note that the volume expansion of the silicon electrode during lithiation can determined by in-operando neutron reflectometry with high accuracy [5,9]. Additional experiments with classical methods of microstructure analysis (like electron microscopy) e. g. done before and after cycling will give no significant new aspects concerning the detected non-linear volume expansion during lithiation.

2. Experimental details

Electrochemical lithiation was done using a home-made closed electrochemical cell constructed for use at neutron facilities as basically described in ref. [17]. A large area thin film electrode was prepared for the NR experiments. The working electrode was made of a 1 cm thick support quartz block, which was coated by a 400 nm copper layer as a back contact and current collector. The active electrode material is an amorphous silicon film with a thickness of about 40 – 50 nm, which was
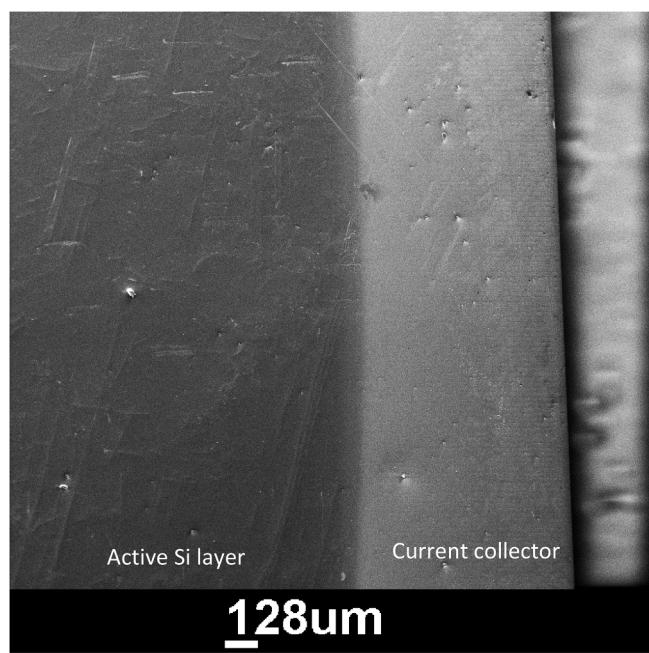

Fig. 1. SEM image (top view) of the electrode after sputter deposition. The darker region on the left side belongs to an area where the active silicon layer is deposited on top of the copper current collector while the brighter region on the right side is the copper current collector without silicon.

deposited by r.f. magnetron sputtering on top of the copper. The thickness listed is an estimation only as known from similar deposition runs and was not exactly determined. The counter electrode was made of metallic lithium (1.5 mm foil, 99.9%, Alfa Aesar). Additionally, a separator with a thickness of 20 μm (Brückner Maschinenbau, Germany) was introduced between the two electrodes. As electrolyte, propylene carbonate (Sigma Aldrich, anhydrous, 99.7%) with 1 M $LiClO_4$ (Sigma Aldrich, battery grade) was used. The electrochemical cell was assembled within an argon filled glove-box (water content < 0.1 ppm, oxygen content < 0.1 ppm).

Secondary Electron Microscopy (SEM) was done with a CamScan 44 microscope (Obducat CamScan Ltd). A SEM image (top view) of the electrode after sputter deposition before incorporation into the electrochemical cell is given in Fig. 1. The image shows the overall morphology of a thin film with a smooth surface. A characteristic pore structure is not present. High resolution images (not shown) did not reveal the presence of nano-pores down to the sub-micrometer range.

Electrochemical lithiation was carried out using a computer controlled potentiostat (BioLogic, model SP-50). Potentiostatic lithiation was done step-by-step at potentials of 0.45, 0.28, 0.19 and 0.06 V vs. reference electrode, while the open-circuit potential of the pre-cycled electrode was about 1.0 V. The potentiostatic pre-cycling procedure was also done step-by-step at potentials of 1 V, 0.45, 0.28, 0.19 and 0.06 V (lithiation) and 0.3, 0.5 and 1 V (delithiation). After application of the potential, the resulting current was recorded as a function of time until significant modifications are no longer observed. The sequence of applied potential and the response of the current during lithiation is shown in Fig. 3(a).

In-situ NR was performed at the Time-of-Flight reflectometer Amor (Paul-Scherrer-Institute Villigen). Using the Selene option (focusing reflectometry) it is possible to record reliable reflectivity patterns up to 0.08 Å^{-1} within an acquisition time of 1–2 min for each. Details can be found in [5,18,19]. Data analysis was performed using Parratt's recursion formula within the Motofit software package [20] by fitting the measured NR patterns.

3. Results and discussion

Fig. 2(a) shows a neutron reflection pattern in the initial state at the open-circuit potential recorded after assembling the cell, filling with electrolyte and pre-cycling the electrode for one cycle in order to establish an equilibrium state. The pattern shows slight fringes, which result from the interference of neutrons reflected at the Cu/Si and Si/electrolyte interfaces. The NR pattern was fitted by the program Motofit using a layer-model as described in detail in ref. [17]. A thickness of (43.4 ± 2.5) nm is found for the amorphous silicon layer. The neutron scattering length densities (SLD) are $(4.15 ± 0.20) × 10^{-6}$ Å^{-2} for the SiO_2 support, $(6.77 ± 0.20) × 10^{-6}$ Å^{-2} for the copper layer and $(1.00 ± 0.35) × 10^{-6}$ Å^{-2} for the amorphous silicon layer. The SLD of the silicon layer is in agreement to the results of other measurements on silicon electrodes after pre-cycling [19]. Error limits correspond to a 10% increase of χ^2 of the best fit with respect to the fitted parameter only. For the SLD of the electrolyte we used a fixed value of $1.75 × 10^{-6}$ Å^{-2} [5] and for the interface roughness between SiO_2/Cu, Cu/Si, and Si/electrolyte constant values of 0.5, 1.0 and 0.5 nm, respectively. The existence of a possible Solid Electrolyte Interphase (SEI) at the surface was not incorporated into the model.

Characteristic examples of neutron reflection patterns recorded in-operando continuously during lithiation are displayed in Fig. 2(b, c, d). The neutron reflection patterns are modified during electrode lithiation and the number of fringes in a given scattering vector interval increases. This indicates the modification of layer thickness and volume due to the incorporation of lithium into the electrode [5,9]. The changed density/SLD within the electrode layer alters the amplitude of the oscillations. The silicon electrode layer thickness is extracted from the reflectivity measurements during lithiation by fitting again the patterns with the program Motofit. The resulting reflectivity curves are also shown in Fig. 2 as red lines. The SLD and thickness of the copper layer and the SLD of the quartz substrate and the electrolyte of the lithiated samples are fixed to the values of the initial state. As free fit parameters, the thickness and SLD of the lithiated silicon layer are used. As shown in ref. [5,9] the layer thickness can be correctly extracted from the reflectivity data assuming a single Li_xSi layer that is continuously expanded during lithiation. Here, the extraction of the correct layer thickness is independent of the underlying lithiation model. Let us assume two types of models: (a) a homogeneous model where the concentration x in Li_xSi is constant within the electrode and increases during lithiation and (b) a heterogeneous model where a phase with a high lithium concentration (e.g. Li_4Si) enters the silicon electrode from the surface as a function of lithiation time (abrupt change of the Li concentration in the electrode). Both models of Li filling result in the same thickness/volume change as long as the same amount of Li is introduced (see ref. [5,9]). We note that the chosen analysis does not necessarily require a homogeneous lithiation mechanism to be present. Instead, a heterogeneous mechanism is more likely, but much complicates the analysis procedure [5]. Consequently, the obtained SLD might be strongly averaged value.

In Fig. 3(b) the variation of the layer thickness as extracted from the fits is displayed as a function of lithiation time together with the lithiation current exemplarily for the case of a potential of 0.19 V. After fixing the potential to the given value, a current flow is established that decreases in absolute values as a function of lithiation time from about 1.5 mA (established within seconds after applying the potential) down to 5 μA (red curve). At the same time the layer thickness increases with the same functional dependence (dots). This indicates that the incorporation of Li into the electrode scales with the current. A similar behaviour is observed for all other potentials. The measurement was stopped after two hours, while the current is no longer significantly modified. Shown in Fig. 3(b) are the layer thickness L for reflectivity patterns recorded for a time period of 1 min (up to 20 min of overall lithiation time) and 5 min respectively. For the second case, five reflectivity patterns were summed up and the thickness is extracted out of
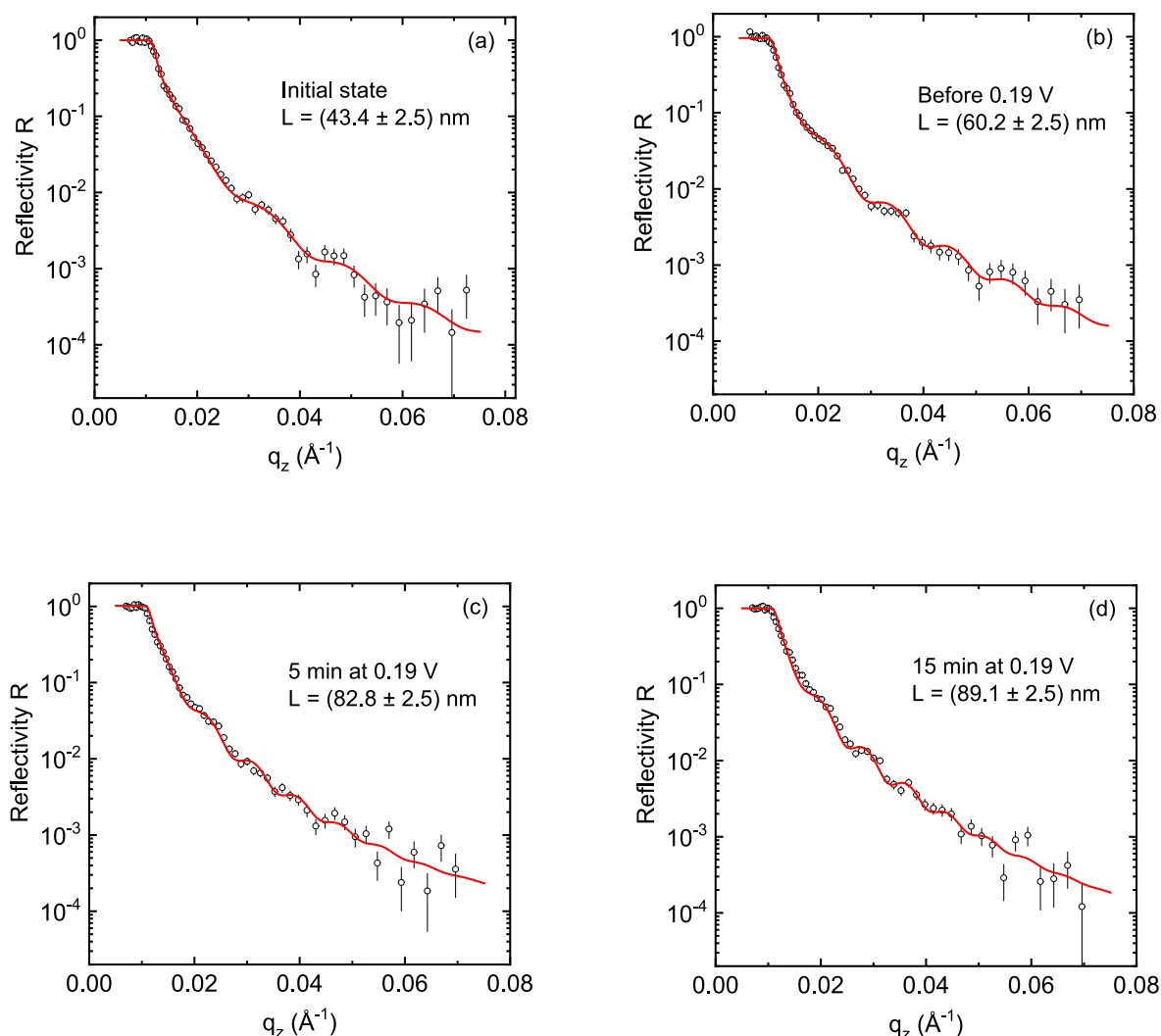
Fig. 2. Neutron reflectometry patterns (open circles) for (a) the initial state, (b) before a potential of 0.19 V was applied, (c) after 5 min at 0.19 V and (d) after 15 min at 0.19 V. Also shown are the fitting results using the program Motofit (red lines). The thicknesses extracted by fitting are indicated. (For interpretation of the references to colour in this figure legend, the reader is referred to the web version of this article.)

this. This was done in order to reduce statistical errors at times where the thickness is modified only slightly (20–120 min). The thicknesses obtained for the 1 and 5 min data, respectively, are identical within error limits. Fig. 3(b) shows that the modification of layer thickness follows the modification of the current. High currents also give rise to high rates of lithiation and high modifications of the thickness. With increasing time all these quantities become lower until an equilibrium state is reached. The observation that the modification of the volume follows the modification of the current brings us to the problematic situation that a high rate of lithiation which is desirable to realize short charging times is coupled to a high increase in volume what is detrimental for long-term performance. Both effects have to be payed attention to by realizing advanced battery designs.

For further analysis, we assume that during Li incorporation the initial silicon layer is expanded mainly in the direction perpendicular to the surface. Expansion in the direction parallel to the surface is strongly suppressed due to the adhesion of silicon to the substrate. Consequently, we assume a negligible length expansion parallel to the surface and the relative change of the thickness of the Li_xSi layer, L, is assumed to be identical to the volume change, V, according to $L/L_0 = V/V_0$, where the index 0 refers to the initial value ($L_0 = 43.4$ nm).

In Fig. 4(a) the relative volume change is plotted as a function of x in Li_xSi for 0.45, 0.28, 0.19 and 0.06 V. The quantity x is calculated

from plots as shown in Fig. 2 by numerical integration according to

$$x = \int_0^t I(t')dt' \frac{M_{Si}}{F\, m_{Si}} \tag{1}$$

where t is the lithiation time, I(t) the current shown for example in Fig. 3(b), $m_{Si} \approx 1.2 \times 10^{-4}$ g is the actual silicon electrode mass, $F = 96487$ C/mol is the Faraday constant, and $M_{Si} = 28.09$ g/mol is the molar mass of silicon.

As shown in ref. [5,9] for galvanostatic lithiation there is a linear relationship between the quantities V/V_0 and x (for $x > 0.5$ and a current density $< 5\ \mu A/cm^2$). Such a correlation is also observed here in good approximation (line in Fig. 4(a)) if only values are plotted corresponding to long lithiation times where the current is negligible small (see e. g. Fig. 3(b) for about 120 min). At this state of charge, the system is more or less in equilibrium. However, in-between the starting and end point of each constant potential measurement, a strong non-linear dependence between relative volume and deposited charge (given as x) is observed. If a new potential is applied to the electrode, like 0.19 V in Fig. 3(b), high currents flow up to 1.5 mA corresponding to lithiation rates of 3C. Such high currents seem to lead to a higher volume expansion than expected from the volume change vs. charge state for galvanostatic experiments (the continuous curve in Fig. 4(a)). As the current decreases as a function of time, the rate of volume
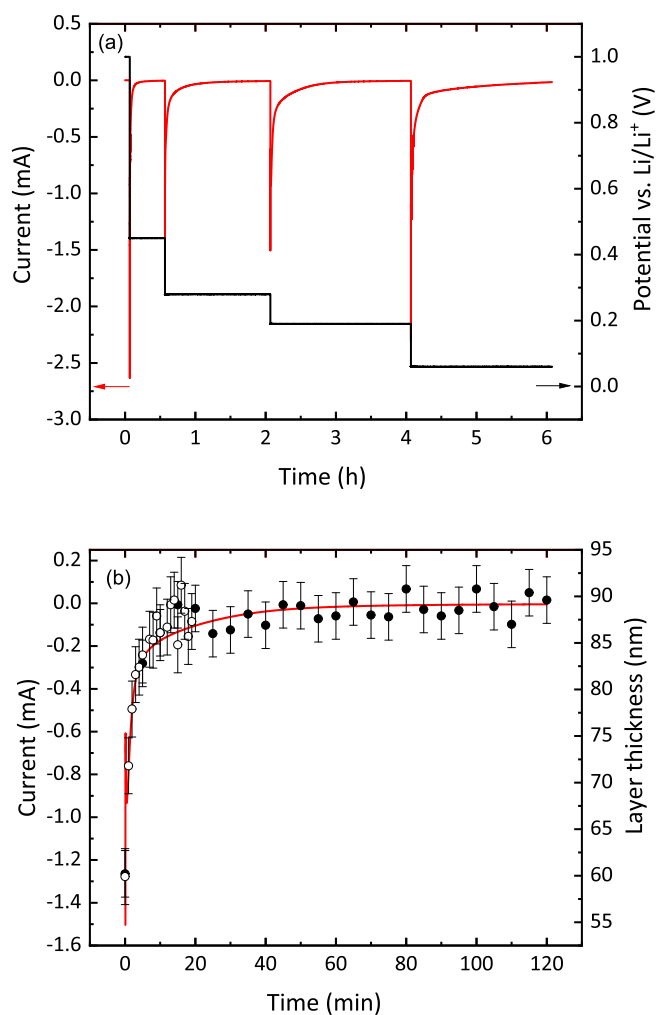
Fig. 3. (a) Current (red line) and potential (black line) vs. absolute time for the lithiation experiments described. (b) Current (red line) and electrode thickness (dots) vs. lithiation time for a fixed potential of 0.19 V. Open symbols refer to a recording time for each reflectivity curve of 1 min, while closed symbols refer to 5 min. A current of 1 mA corresponds to a current density of 78 μA/cm². The lithiation time in (b) is normalized to zero at the beginning of the potential jump. (For interpretation of the references to colour in this figure legend, the reader is referred to the web version of this article.)

Fig. 4. (a) Relative volume V/V_0 plotted against x in Li_xSi as obtained during potentiostatic lithiation measurements at the given potentials. Open circles refer to a recording time for each reflectivity curve of 1 min, while open squares refer to 5 min. Error limits are less than the symbols. (b) Corresponding SLD plotted against x in Li_xSi.

expansion slows down. The in-operando determined rate of volume increase (Fig. 4(a)) shows a higher value for higher currents. This behaviour is present for each of the potentiostatic lithiation curves. Note that in ref. [13] deviations from linearity in the volume vs. capacity (proportional to x) curve were observed. However, analysis was done on an electrode composed of silicon powder particles mixed with carbon black and polyvinylidene difluoride and not for a pure thin Si film as in our case. This might cause the differences during galvanostatic lithiation.

The SLD extracted from the patterns during fitting is displayed in Fig. 4(b). Due to high error limits attributed to the measurement data using the definition given above, an analysis is difficult. It can be stated that the SLD decreases from an initial value of about 1×10^{-6} Å^{-2} to a final value around zero during lithiation. This decrease reflects that Li is incorporated into the electrode leading to the volume expansion observed. Further meaningful conclusions cannot be drawn from this behaviour due to the high error limits.

A possible explanation for the observed results on volume expansion might be that the high currents occurring during the initial state of each experiment at a defined constant potential are the reason for the disproportionate volume expansion. High currents are associated with a
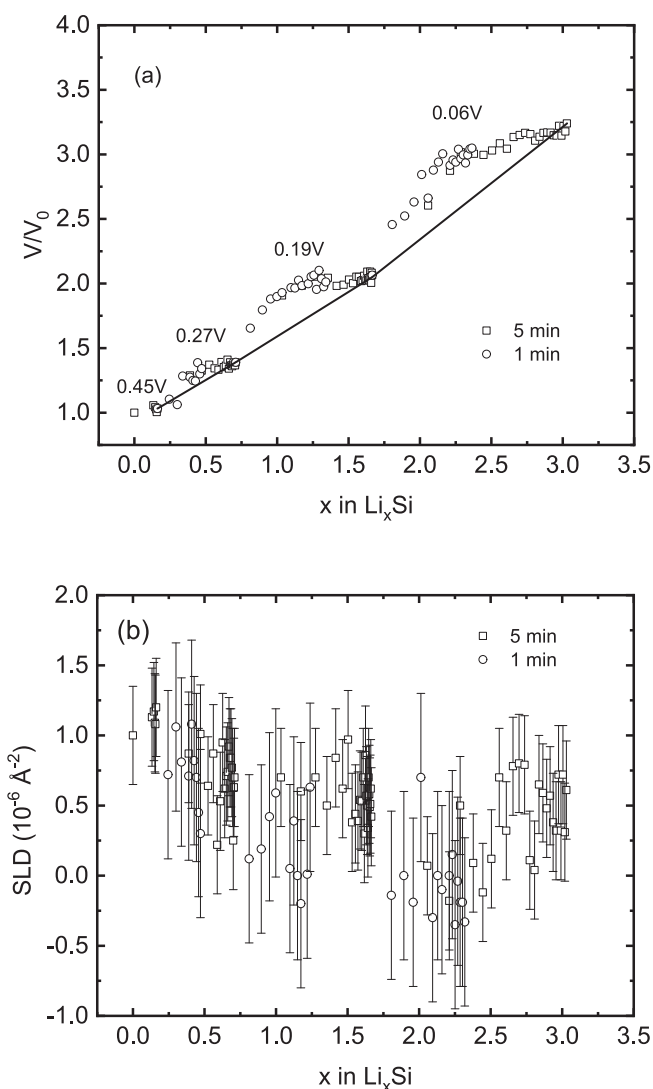
high rate of lithiation meaning a high flux of Li ions entering the electrode in short time intervals. This has the consequence that the atoms in the electrode cannot properly re-arrange in order to form a state of lowest energy and a non-relaxed solid in a non-equilibrium state is formed. Such a state is very likely associated with the formation of free volumes (for example nano-scaled pores or regions of lower density) within the active silicon material. This gives rise to higher relative volumes than expected for a proper arrangement of atoms occurring during galvanostatic lithiation.

Such a non-equilibrium state can relax by structural relaxation due to a re-arrangement and migration of Li ions in order to form an optimised arrangement of the amorphous structure. The diffusivity of Li in lithiated amorphous silicon close to room temperature is in the order of 10^{-17}–10^{-18} m²/s [21] and even less for Li_xSi x $<$ 0.1 [22] (extrapolated). This means for a time period of about 5 min after starting where the highest currents and the strongest increase of volume is observed, the Li atoms can move by diffusion only on a length scale in the order of the electrode thickness or less and a proper re-arrangement of atoms is not possible. If the lithiation current and the Li flux from the surface decreases no further or less free volumes are formed. Now the

system has time to re-arrange by diffusion during a longer time period of two hours. A proper re-arrangement of atoms and the formation of a relaxed atomic structure become now possible.

Note that described explanation is very tentative. It is important to get further evidences on this point during future experiments for example by Secondary Ion Mass Spectrometry experiments as described in ref. [5] for galvanostatic lithiation. Further investigations with neutron reflectometry, like galvanostatic measurements at very high lithiation rates and potentiostatic measurements during delithiation and as a function of electrode thickness and cycle number are also planned for the future. The latter point is necessary to get an impression of the significance of our findings for the long term performance of Si electrodes. If the same results will be obtained, the suggestion for battery design would be to avoid high currents what will limit disproportional volume expansion detrimental for the electrode. The incorporation of silicon into a buffer material like e.g. carbon might also help to limit volume expansion.

4. Conclusion

In-operando neutron reflectometry was applied in order to determine the volume expansion of amorphous silicon thin film electrodes in real-time during potentiostatic lithiation at potentials of 0.45, 0.28, 0.19 und 0.06 V vs Li/Li$^+$. It is found that the volume expansion of the electrode due to Li incorporation shows a strong non-linear behavior as a function of x in Li$_x$Si in contrast to galvanostatic cycling. We explain this effect with the assumption that for high current densities occurring at the beginning of the lithiation process free volumes are created in the electrode material leading to disproportionate volume expansion. If current densities decrease during further lithiation, no further free volumes are formed and a structural rearrangement can take place by diffusion.

CRediT authorship contribution statement

Harald Schmidt: Conceptualization, Formal analysis, Writing - review & editing, Supervision, Project administration, Funding acquisition. **Bujar Jerliu:** Investigation, Formal analysis, Writing - review & editing. **Erwin Hüger:** Investigation, Writing - review & editing. **Jochen Stahn:** Investigation, Software, Methodology.

Declaration of Competing Interest

The authors declare that they have no known competing financial interests or personal relationships that could have appeared to influence the work reported in this paper.

Acknowledgements

References

[1] M.T. McDowell, S.W. Lee, W.D. Nix, Y. Cui, Understanding the lithiation of silicon and other alloying anodes for lithium-ion batteries, Adv. Mater. 25 (2013) 4966–4985, https://doi.org/10.1002/adma.201301795.

[2] X. Yuan, H. Liu, J. Zhang, Lithium-ion Batteries: Advanced Materials and Technologies, CRC Press, Boca Raton, FL, 2012.

[3] L. Zhao, D.J. Dvorak, M.N. Obrovac, Layered amorphous silicon as negative electrodes in lithium-ion batteries, J. Power Sources 332 (2016) 290–298, https://doi.org/10.1016/j.jpowsour.2016.09.124.

[4] Y. Tan, K. Wang, Silicon-based anode materials applied in high specific energy lithium-ion batteries: a review, J. Inorg. Mater. 34 (2019) 349, https://doi.org/10.15541/jim20180347.

[5] D. Uxa, B. Jerliu, E. Hüger, L. Dörrer, M. Horisberger, J. Stahn, H. Schmidt, On the lithiation mechanism of amorphous silicon electrodes in Li-ion batteries, J. Phys. Chem. C 123 (2019) 22027–22039, https://doi.org/10.1021/acs.jpcc.9b06011.

[6] V.A. Sethuraman, M.J. Chon, M. Shimshak, V. Srinivasan, P.R. Guduru, In situ measurements of stress evolution in silicon thin films during electrochemical lithiation and delithiation, J. Power Sources 195 (2010) 5062–5066, https://doi.org/10.1016/j.jpowsour.2010.02.013.

[7] N. Yuca, O.S. Taskin, E. Arici, An overview on efforts to enhance the Si electrode stability for lithium ion batteries, Energy Storage 2 (2020) e94, , https://doi.org/10.1002/est2.94.

[8] J. Wu, et al. Recent progress in advanced characterization methods for silicon-based lithium-ion batteries, Small Methods 3 (2019) 1900158.

[9] B. Jerliu, E. Hüger, L. Dörrer, B.-K. Seidlhofer, R. Steitz, V. Oberst, U. Geckle, M. Bruns, H. Schmidt, Volume expansion during lithiation of amorphous silicon thin film electrodes studied by in-operando neutron reflectometry, J. Phys. Chem. C 118 (2014) 9395–9399, https://doi.org/10.1021/jp502261t.

[10] C.R. Becker, K.E. Strawhecker, Q.P. McAllister, C.A. Lundgren, In situ atomic force microscopy of lithiation and delithiation of silicon nanostructures for lithium ion batteries, ACS Nano 7 (2013) 9173–9182, https://doi.org/10.1021/nn4037909.

[11] L.Y. Beaulieu, T.D. Hatchard, A. Bonakdarpour, M.D. Fleischauer, J.R. Dahn, Reaction of Li with alloy thin films studied by in situ AFM, J. Electrochem. Soc. 150 (2003) A1457, https://doi.org/10.1149/1.1613668.

[12] B. Breitung, P. Baumann, H. Sommer, J. Janek, T. Brezesinski, In situ and operando atomic force microscopy of high-capacity nano-silicon based electrodes for lithium-ion batteries, Nanoscale 8 (2016) 14048–14056, https://doi.org/10.1039/C6NR03575B.

[13] K. Dong, H. Markötter, F. Sun, A. Hilger, N. Kardjilov, J. Banhart, I. Manke, In situ and operando tracking of microstructure and volume evolution of silicon electrodes by using synchrotron X-ray imaging, Chem. Sus. Chem. 12 (2019) 261–269, https://doi.org/10.1002/cssc.201801969.

[14] J. Duay, K.W. Schroder, S. Murugesan, K.J. Stevenson, Monitoring volumetric changes in silicon thin-film anodes through in situ optical diffraction microscopy, ACS Appl. Mater. Interfaces 8 (2016) 17642–17650, https://doi.org/10.1021/acsami.6b03822.

[15] C. Cao, H.-G. Steinrück, B. Shyam, K.H. Stone, M.F. Toney, In situ study of silicon electrode lithiation with X-ray reflectivity, Nano Lett. 16 (2016) 7394–7401, https://doi.org/10.1021/acs.nanolett.6b02926.

[16] S. Choi, T. Bok, J. Ryu, J.-In Lee, J. Cho, S. Park, Revisit of metallothermic reduction for macroporous Si: compromise between capacity and volume expansion for practical Li-ion battery, Nano Energy 12 (2015) 161–168, https://doi.org/10.1016/j.nanoen.2014.12.010.

[17] B. Jerliu, L. Dorrer, E. Huger, G. Borchardt, R. Steitz, U. Geckle, V. Oberst, M. Bruns, O. Schneider, H. Schmidt, Neutron reflectometry studies on the lithiation of amorphous silicon electrodes in lithium-ion batteries, Phys. Chem. Chem. Phys. 15 (2013) 7777–7784, https://doi.org/10.1039/c3cp44438d.

[18] J. Stahn, A. Glavic, Focusing neutron reflectometry: implementation and experience on the TOF-reflectometer Amor, Nucl. Instrum. Methods Phys. Res., Sect. A 821 (2016) 44–54, https://doi.org/10.1016/j.nima.2016.03.007.

[19] B. Jerliu, E. Hüger, M. Horisberger, J. Stahn, H. Schmidt, Irreversible lithium storage during lithiation of amorphous silicon thin film electrodes studied by in-situ neutron reflectometry, J. Power Sources 359 (2017) 415–421, https://doi.org/10.1016/j.jpowsour.2017.05.095.

[20] A. Nelson, Co-refinement of multiple-contrast neutron/X-ray reflectivity data using Motofit, J. Appl. Crystallogr. 39 (2006) 273–276, https://doi.org/10.1107/S0021889806005073.

[21] J. Li, X. Xiao, F. Yang, M.W. Verbrugge, Y.-T. Cheng, Potentiostatic intermittent titration technique for electrodes governed by diffusion and interfacial reaction, J. Phys. Chem. C 116 (2012) 1472–1478, https://doi.org/10.1021/jp207919q.

[22] F. Strauß, L. Dörrer, M. Bruns, H. Schmidt, Lithium tracer diffusion in amorphous LixSi for low Li concentrations, J. Phys. Chem. C 122 (2018) 6508–6513, https://doi.org/10.1021/acs.jpcc.7b12296.